Pramāṇa, Vol. 11, No. 5, November 1978, pp. 619–637, © printed in India

Scale breaking in neutrino scattering

D P ROY, S PARANJAPE, P N PANDITA and D K CHOUDHURY
Tata Institute of Fundamental Research, Bombay 400 005

MS received 10 July 1978

Abstract. We consider two types of scale breaking models—one based on asymptotically free gauge theory and the other phenomenological—which have already been fitted to the electron and muon data. Their predictions for the neutrino scattering are worked out and the sensitivity on the model parameters and the input electron data studied. The effects of scale breaking at very low Q^2 and of a finite longitudinal cross-section are incorporated in analogy with *ep* data. The predictions are compared with the recent neutrino scattering data.

Keywords. Asymptotically free gauge theory; phenomenological scale breaking; quark and gluon distributions; longitudinal and transverse cross-sections; SU(3) breaking.

1. Introduction

The most recent neutrino data (Holder *et al* 1977; Bosetti *et al* 1977; Barish *et al* 1977) seem to rule out any violent scale breaking, which was reported by an earlier experiment (Benevenuti *et al* 1976) and were associated with right handed excitation of new quarks. However, a part of the new data (Bosetti *et al* 1977; Barish *et al* 1977) is suggestive and the rest (Holder *et al* 1977) is, at least, consistent with a more modest scale breaking of 10–20%. This is also the size of scale breaking observed in deep inelastic electron (Riordon *et al* 1975) and muon (Anderson *et al* 1976, 1977) scattering. Several models have been constructed to describe scale breaking effects of this magnitude—some of them based on asymptotically free gauge theory (AFT) (Altarelli 1976; Barnett *et al* 1976; Gluck and Reya 1976; Buras and Gaemers 1978) and others of purely phenomenological type (Perkins *et al* 1977; Karliner and Sullivan 1977). Thus the new neutrino data are likely to provide a very useful testing ground for these scale breaking models. Of course, there are still differences amongst these data (Holder *et al* 1977; Bosetti *et al* 1977; Barish *et al* 1977), on a quantitative level, which are to be settled before a detailed comparison is possible. It is useful nonetheless to work out the characteristic predictions of these models for neutrino scattering and check their sensitivity to the underlying parameters and the various assumptions involved in the light of the available data. The present paper is devoted to this exercise.

We concentrate on a specific model each, of the AFT and the phenomenological type, chosen by the twin criteria of simplicity and the level of success in describing the electron and (muon) scale breaking. These are the models of Buras and Gaemers (1977) (model I) and of Perkins *et al* (1977) (model II). For the AFT based model I,

we check the dependence on the scale breaking parameter and the gluon distribution. We also consider combinations of experimental quantities which are independent of the gluon distribution. For the phenomenological model II, the scale breaking parameters are more flexible. We vary them within the lattitude allowed by the electron data and check the resulting variation of the neutrino cross-sections.

The above models do not take account of the scale breaking in the low Q^2 region ($<1{\cdot}8$ GeV^2). Since this region accounts for about half the neutrino cross-sections in the energy range of 10–30 GeV, and one has only Q^2 integrated neutrino data, no meaningful comparison with these models is possible, without an estimate of the low Q^2 scale breaking effect. We try to estimate this effect by assuming the neutrino structure functions to have the same Q^2 dependence in this region, as that observed for the electron structure functions.

The above models also assume the Callan-Gross relation, i.e. a zero longitudinal to transverse cross-section ratio. However, a recent SLAC measurement gives a sizeable value for this ratio, although still with rather large uncertainties. We have tried to estimate this effect by assuming the same value for the ratio of the corresponding neutrino structure functions (Barger and Phillips 1978).

We have also studied the effect of SU(3) breaking in the parton sea on the neutrino scattering predictions. One possible source of scale breaking ignored here is the left handed excitation of quarks heavier than charm, e.g. the ones associated with the 9·5 GeV upsilon reported recently (Lederman *et al* 1977). The corresponding threshold is well within the energy range of these neutrino data. However, the weak interaction properties of these objects are completely unknown, and even their existence rather uncertain. Therefore, it would be premature at this stage to speculate on their contribution to scale breaking.

The formalism and the conventions are summarised in the appendix. It contains the formulae relating the cross-sections to the quark distribution functions and explicit expressions for these distribution functions, for the two scale breaking models under consideration. It also includes the formulae, relevant for the low Q^2 scale breaking and the longitudinal cross-section contribution. Most of these formulae, of course, exist in the literature and are familiar to the experts in the field. However, we felt their inclusion would help the general readability of the paper and also enable any interested to crosscheck our results.

2. Results

We shall first compare the models with some *ep* data and then discuss their predictions for the neutrino cross-sections.

2.1. *AFT scale breaking (model I)*

In this model (Buras and Gaemers 1978) the sea term rises and the valence term falls with increasing Q^2, which is in nice qualitative agreement with the observed rise of the electron and muon structure functions at small x and their fall at large x. Moreover, the model predicts both the valence and sea distributions to shrink with increasing Q^2. Thus over regions dominated by valence (sea) the decrease (increase) is predicted to be sharper with increasing (decreasing) x-again in agreement with data.

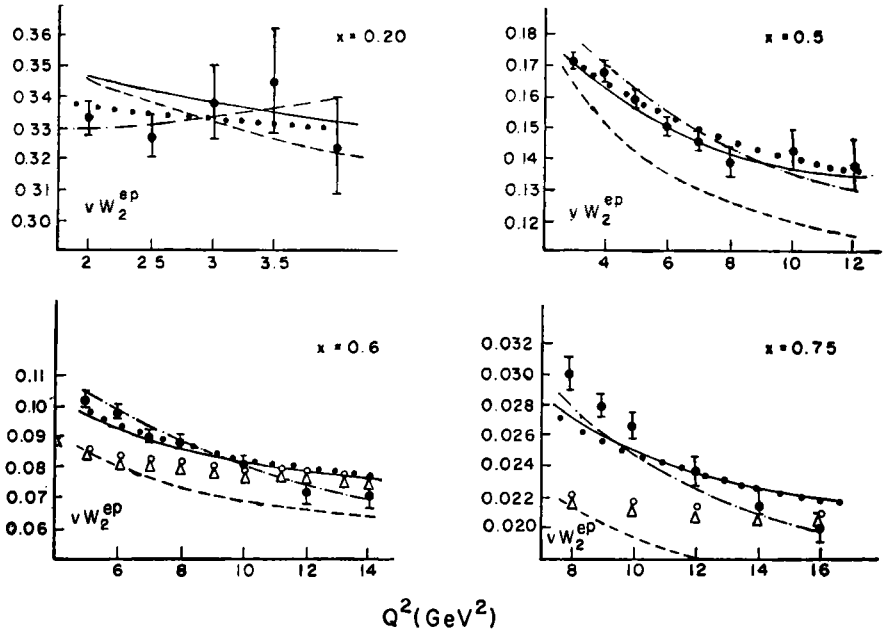

Figure 1. The *ep* structure function data compared with the predictions of models I, II and IA. The model I predictions are the solid and dashed lines corresponding to $\Lambda=0{\cdot}3$ and $0{\cdot}5$, and the model II predictions are the dot dashed and dotted lines corresponding to the original and modified parametrisations of (A.19) and (A.21). The model IA predictions at $x = 0{\cdot}6$ and $0{\cdot}75$ are shown by circles ($\Lambda=0{\cdot}3$) and triangles ($\Lambda=0{\cdot}5$).

On a more quantitative level, however, the data seem to indicate a somewhat faster shrinkage of the valence and sea distributions than this model. Thus in figure 1 the model prediction (solid lines) falls somewhat less sharply than the data, at the large values of $x=0{\cdot}6$ and $0{\cdot}75$. Similarly in the very low x region the model prediction rises less sharply than the muon data (Anderson *et al* 1976, 1977), not shown here. However, the cross-section itself is quite small at large x and the low x muon data has big error bars. Thus, whatever discrepancy there is with the electron and muon data so far available, may not be particularly serious.*

The prediction for the ratio

$$R = \sigma_{\bar{\nu}}/\sigma_{\nu} \tag{1}$$

is shown in figure 2a (solid line). Over the energy range of 30–200 GeV, covered by the recent data, the rise is $\sim$7%. It depends only weakly on the scale breaking parameter—even with the maximal value of $\Lambda=0{\cdot}5$ (dashed line) the corresponding rise is $\sim$8%. Changing the gluon distribution parameter to $G^2=0{\cdot}057$ makes negligible difference (not shown). The high statistics CDHS experiment (Holder *et al* 1977) favours such a slow rise of $\sim$7–8%. On the other hand, both the CIT (Barish *et al* 1977) and the BEBC (Bosetti *et al* 1977) data favour a faster rise of $\sim$25%. But these latter experiments have huge error bars, within which they are compatible with

*It has also been suggested that the discrepancies can be accounted for by the higher order AFT corrections and a modified scaling variable (Buras and Gaemers 1978, Fox 1977).

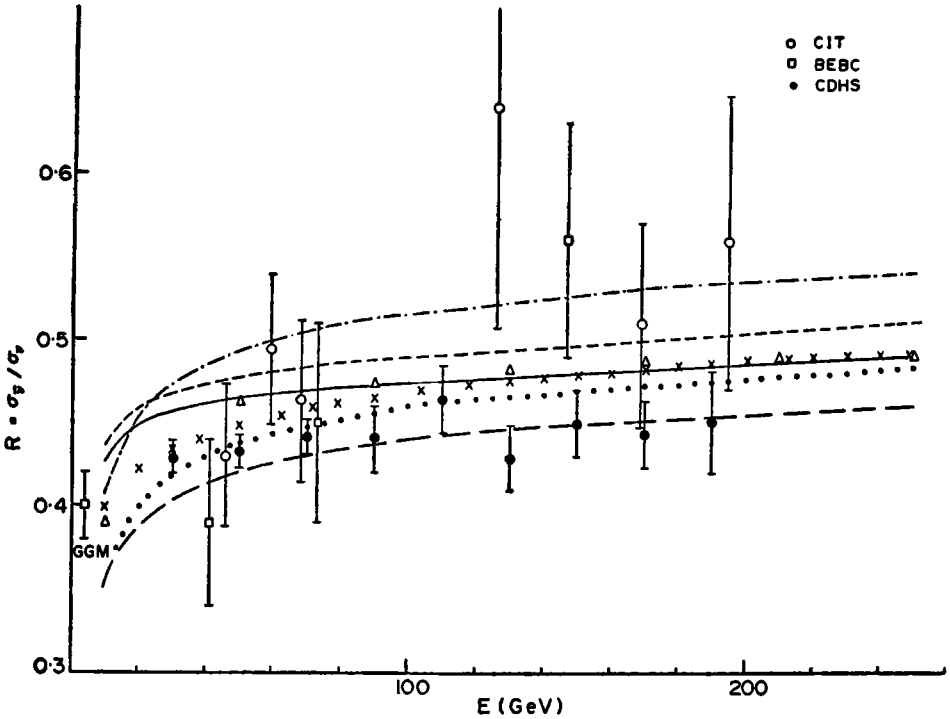

Figure 2a. The GGM, CDHS, BEBC and CIT data on R compared with the model I predictions for $\Lambda=0{\cdot}3$ (solid line) and 0·5 (dashed line). The dotted line refers to the inclusion of low Q^2 scale breaking, whereas long dashed and the dot dashed lines refer to the addition of SU(3) breaking and longitudinal contribution as well (for $\Lambda=0{\cdot}3$). Also shown are the predictions of model IA (crossed line) and a model with low Q^2 scale breaking and longitudinal contribution but no scale breaking at high Q^2 (triangles).

a 7–8% rise, as well. The predicted magnitude of R is systematically above the CDHS and the low energy Gargamelle point (Gargamelle results, corrected for non-isoscalar component in the target, as quoted in Bosetti *et al* 1977) by about 10%. However the magnitude of R is perhaps less significant than the rate of rise, since the former is sensitive to the sea to valence ratio, which is not fixed very precisely by the SLAC data.

The prediction for σ_ν/E (which should be constant in a scaling model) is shown in figure 3a (solid line). Over the energy range 30–200 GeV it goes down monotonically by $\sim$6%. The prediction for $\Lambda=0{\cdot}5$ (dashed line) shows a similar drop $\sim$7%, but the magnitude is lower by $\sim$7%. Changing the gluon distribution to $G^2=0{\cdot}057$ (crosses) evidently makes a negligible difference. Since the CDHS cross-sections are not normalised, we have only CIT and BEBC data on this quantity, which have large error bars. The magnitude of these data points seems to favour the $\Lambda=0{\cdot}5$ curve; but in view of their normalisation uncertainty, it is hard to make a meaningful distinction. One should note that the relative position of the Gargamelle and the CIT (or BEBC) points also suffers from this normalisation uncertainty. The predictions for σ_ν/E are shown in figure 4a. The shape and even the magnitude shows very little dependence on Λ or G^2. They predict a practically flat cross-section over the 30–200 GeV range. In contrast both the CIT and BEBC data favour a rise of $\sim$20%.

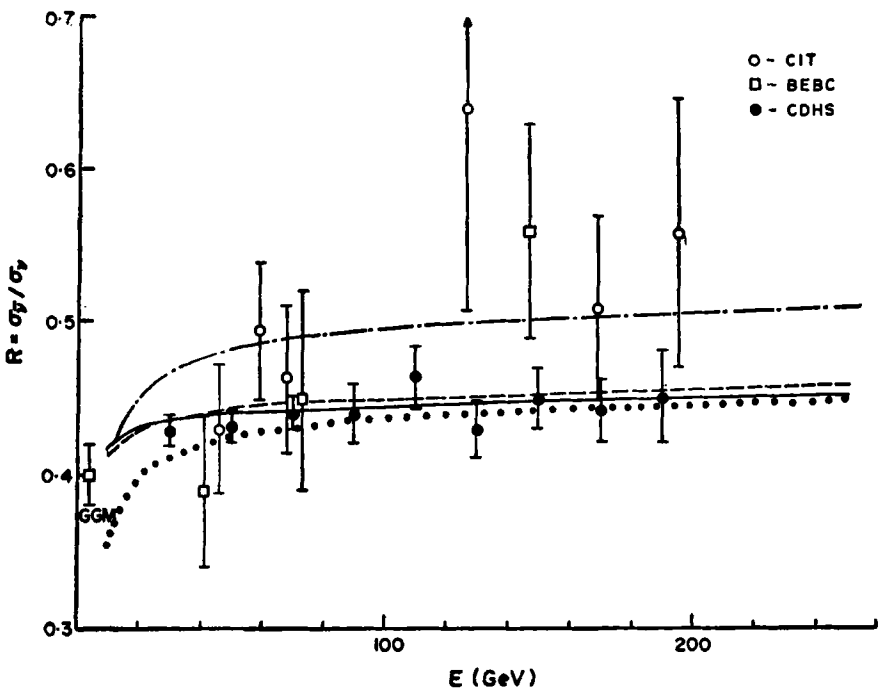

Figure 2b. The GGM, CDHS, BEBC and CIT data on R compared with the model II predictions for the original (solid line) and modified (dashed line parametrisations of (A.19) and (A.21)). The dotted and dot dashed lines again refer to the inclusion of low Q^2 scale breaking and longitudinal contribution (for the original parametrisation).

This is, of course, connected with the larger rise in R favoured by these data. We feel the discrepancy between the prediction and the data in figure 4a rather uncomfortable, although they may be reconciled within the normalisation and statistical uncertainties.

The predictions for $\langle y\rangle_{\bar{\nu}}$ and $\langle y\rangle_{\nu}$ are shown in figure 5a. Over the 30–200 GeV range it predicts a very marginal rise for $\langle y\rangle_{\bar{\nu}} \sim 1\%$ and a marginal fall for $\langle y\rangle_{\nu} \sim 2\%$, with little dependence on Λ (dashed lines) or G^2 (not shown). They agree with the CIT data. Unfortunately the CDHS data (Holder *et al* 1977) on these quantities are not corrected for their acceptance loss for $y > 0{\cdot}85$. This would obviously push down the $\langle y\rangle$ and the effect would be more prominent for ν which has a much larger fraction of events in this region. We believe, this acceptance loss can entirely account for the discrepancy with the CDHS data.

Although the AFT predictions seem to be insensitive to variation in the gluon distribution, within theoretically permissible limits, it may be useful to consider quantities, strictly independent of gluon distribution. The most obvious example of such a 'clean' quantity is the difference $(\sigma_{\nu} - \sigma_{\bar{\nu}})$. Figure 6 compares the predictions for $\Lambda = 0{\cdot}3$ (solid line) and $\Lambda = 0{\cdot}5$ (dashed line) with the CIT and BEBC data. The data seem to favour a faster decrease than the model, but within their large error bars they are compatible with the latter. We do not have the CDHS measurements for this quantity as it depends on normalisation. One can, however, construct quantities,

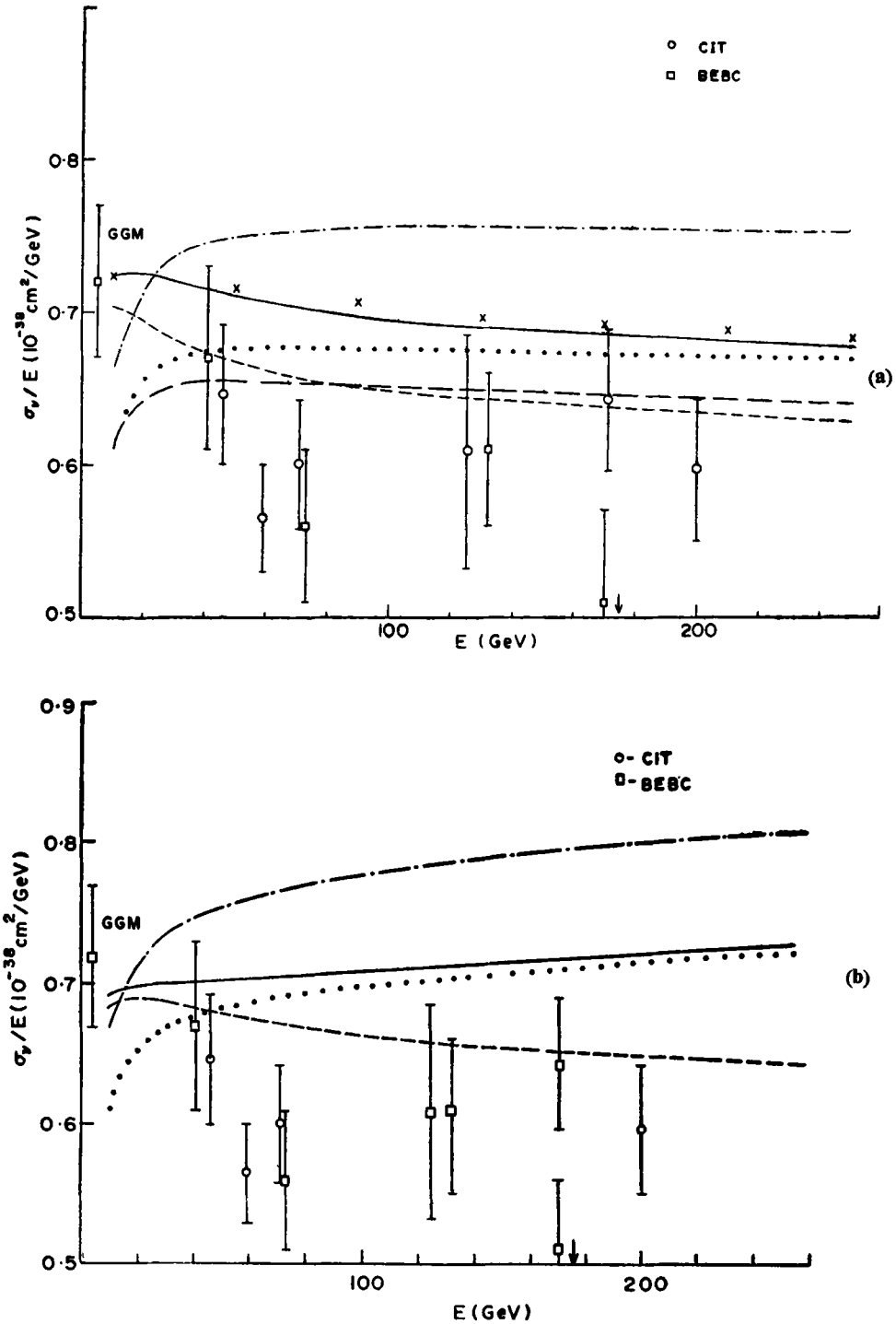

Figure 3. The GGM, BEBC and CIT data on σ_ν/E compared with the model predictions. (a) model I. The description of the curves are same as the previous figure, except that the crosses show the variation with gluon distribution. ($G^2 = 0{\cdot}057$, $\Lambda = 0{\cdot}3$). (b) model II. The descriptions of the curves are same as the previous figure.

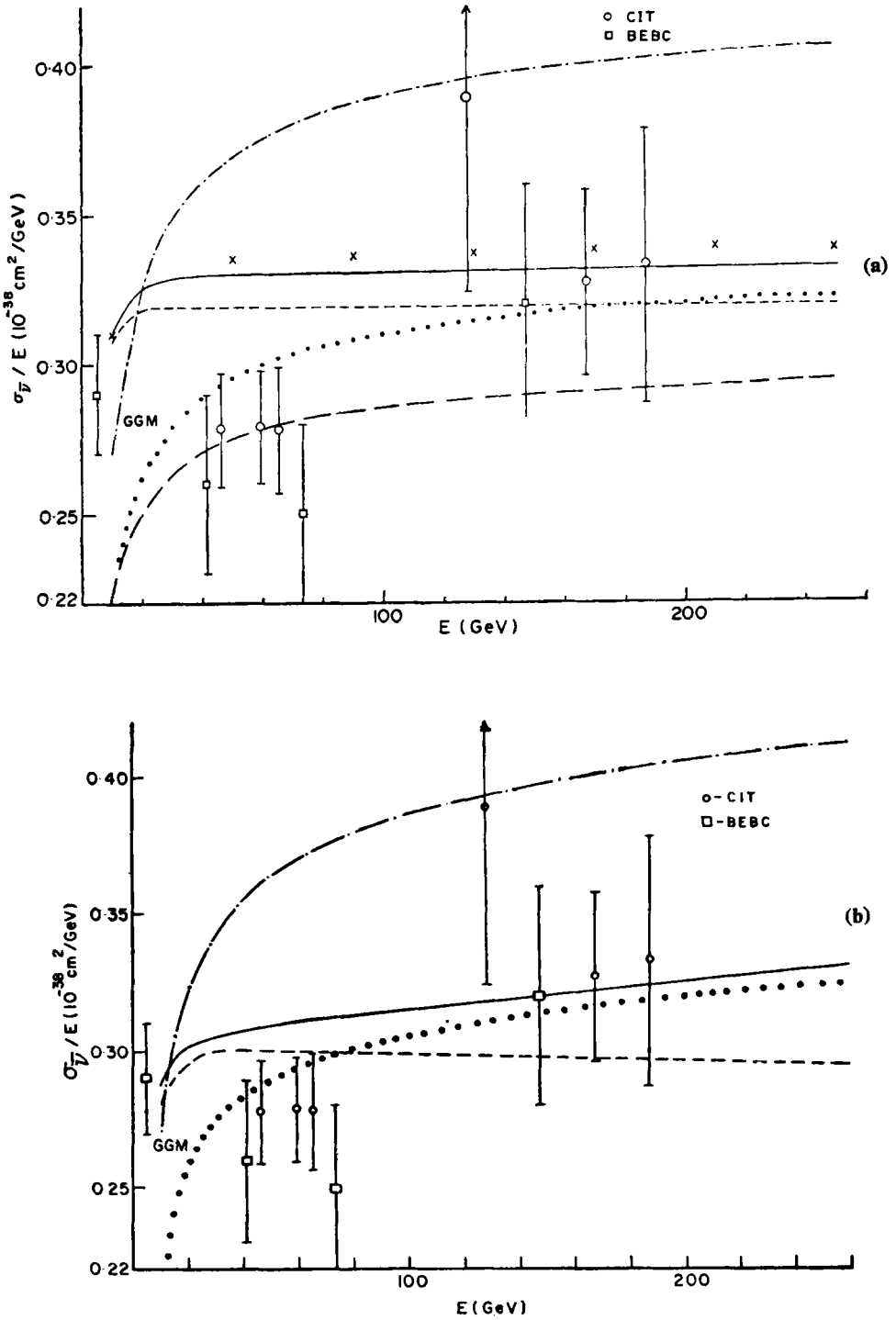

Figure 4. The GGM, BEBC and CIT data on $\sigma_{\bar{\nu}}/E$ compared with the predictions of (a) model I and (b) model II. Descriptions of the curves here and in the subsequent figures are identical to those of the previous figure.

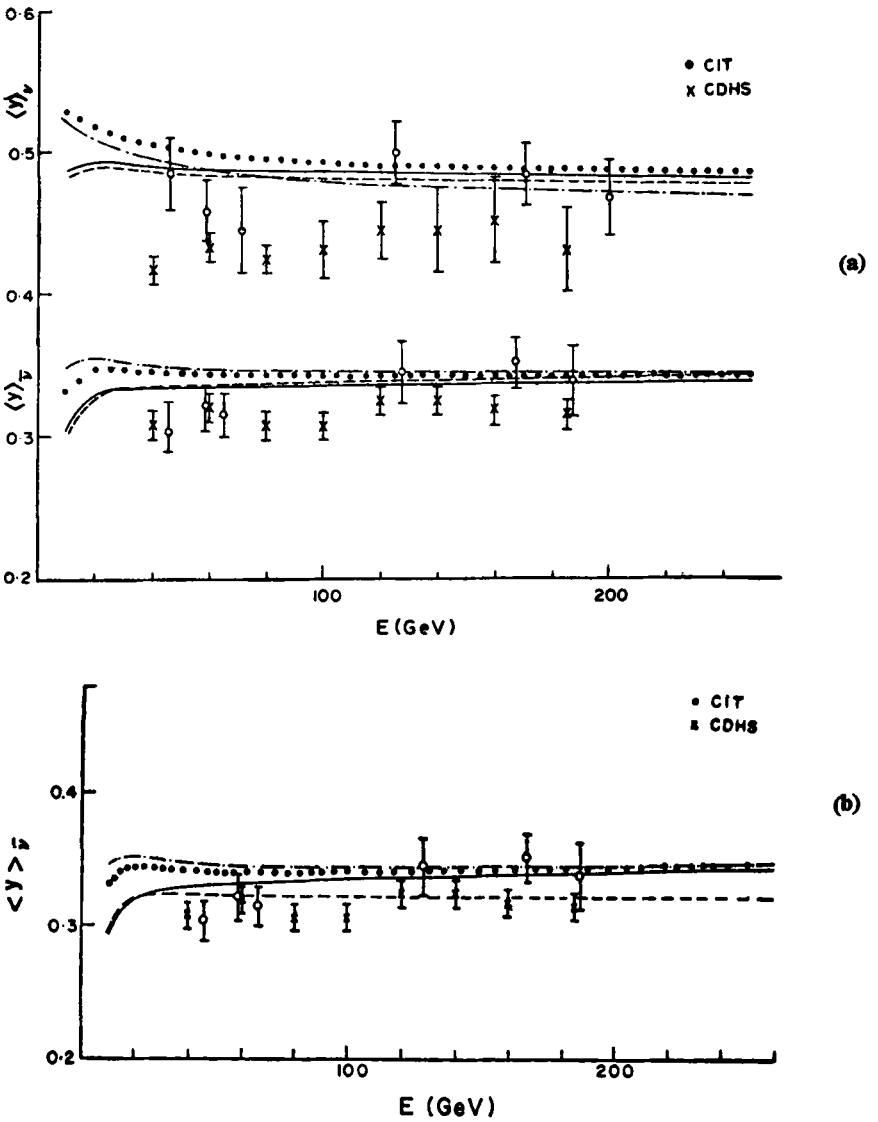

Figure 5 (a). The CIT and CDHS data on $\langle y\rangle_{\nu,\bar{\nu}}$ compared with the predictions of model I. Note that the CDHS data are not corrected for acceptance loss at high y which reduces $\langle y\rangle_{\nu}$ appreciably. (b) The $\langle y\rangle_{\bar{\nu}}$ data compared with the predictions of model II.

independent of gluon distribution which are also normalisation-independent. One such quantity* is

$$P = \frac{\int y\,[(d\sigma^{\nu}/dy - d\sigma^{\bar{\nu}}/dy)]\,dy}{\sigma_{\nu} - \sigma_{\bar{\nu}}} = \frac{\langle y\rangle_{\nu} - \langle y\rangle_{\bar{\nu}} R}{1 - R}. \tag{2}$$

The predictions for this quantity are shown in figure 7 for $\Lambda = 0{\cdot}3$ (solid line) and $\Lambda = 0{\cdot}5$ (dashed line). It is evidently insensitive to Λ and shows only a marginal fall

*We thankfully acknowledge this suggestion from Probir Roy.

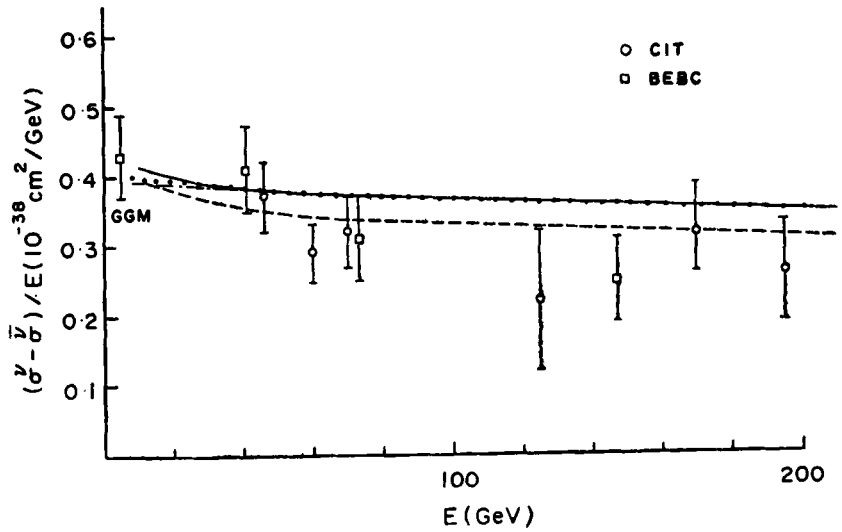

Figure 6. The GGM, CIT and BEBC data on the cross-section difference $(\sigma_\nu - \sigma_{\bar{\nu}})/E$ compared with the predictions of model I.

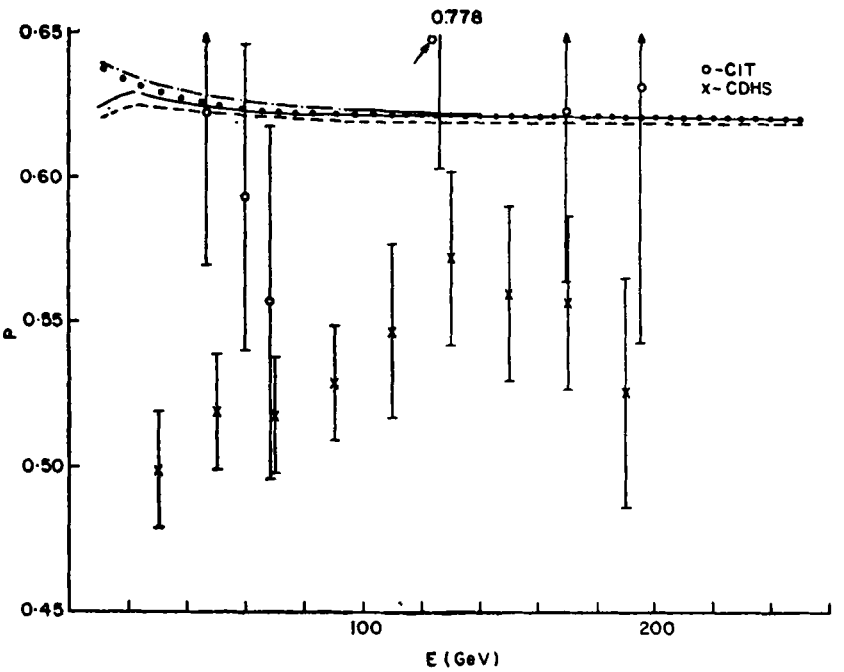

Figure 7. CIT and CDHS data on the quantity P of (2), compared with the predictions of model I. The CDHS data on $\langle y \rangle_{\nu,\nu}$ are not corrected for acceptance loss, which reduces the resulting P substantially.

(~1 %) in the 30–200 GeV region. It is compatible with the CIT data, but the error bars are enormous. Unfortunately, a meaningful comparison with the high statistics CDHS data is not possible as their $\langle y \rangle$ are not corrected for acceptance. The observed discrepancy is simply a reflection of the discrepancy for $\langle y \rangle_\nu$ in figure 5a.

We have also checked the BGP (Barnett *et al* 1976) approximation to the AFT scale breaking (model IA), which has been much discussed in the literature. It assumes the quark distribution functions to have the same Q^2 dependence as the corresponding 1st moments, at all x—i.e. it neglects the shrinkage of the distribution functions with increasing Q^2. It fails badly to describe the electron and muon data in the region of very high and very low x. The first part is illustrated in figure 1 by a comparison with the *ep* data at $x=0{\cdot}6$ and $0{\cdot}75$ (circles and triangles refer to $\Lambda=0{\cdot}3$ and $0{\cdot}5$). In view of this strong discrepancy, its prediction for neutrino cross-sections are of little quantitative significance. We have only shown the prediction for the ratio R in figure 2a (crossed line). One should note that the scale breaking predicted by this model is roughly twice as big as that of a more exact treatment of AFT (solid line).

2.2. *Phenomenological scale breaking (model II)*

This model (Perkins *et al* 1977) fits the electron (muon) data even better than model I, as one can see in figure 1 (dot dashed line). This is not surprising, of course, since it is more flexible. Even assuming a linear x dependence for the power of Q^2 (see eq. (A.19)), there are still two parameters, the slope and the intercept. The range over which they can be varied within the lattitude of the electron (muon) data is illustrated by the modified parametrisation of eq. (A.21). This parametrisation is shown by the dotted line in figure 1. This is, of course, designed to resemble the model I result for *ep* closely, as described in the appendix.

The predictions for the cross-section ratio R is shown in figure 2b, for the original (solid line) and the modified (dashed line) parametrisations of eqs (A.19) and (A.21). The two parametrisations make very similar predictions for R—a 4-5% rise over the 30 to 200 GeV region. Note the rise of R is somewhat slower here than in model I, which simply reflects a slower rise of the sea in this model as discussed later. The magnitude of the predicted R is a little smaller than in model I. The agreement with the CDHS data is embarrassing in the sense that the curves seem to hug the data points all the way through. They, of course, undershoot the high energy BEBC and CIT points; but again within their large error bars they are not incompatible.

The predictions for σ_ν/E are shown in figure 3b. This quantity is more sensitive to the details of parametrisation. The original parametrisation (solid line) predicts a slow rise—by $\sim$3% in the 30–200 GeV range. The modified parametrisation (dashed line) gives a fall—by $\sim$6% over this range. The BEBC and CIT data seem to favour the latter. The corresponding predictions for $\sigma_{\bar\nu}/E$ are shown in figure 4b. The original parametrisation (solid line) predicts a 6% rise over the 30–200 GeV region whereas the modified parametrisation (dashed line) gives a practically flat cross-section over this region. The data points seem to favour the former parametrisation somewhat. Note that the modified parametrisation, designed to resemble the model I results for *ep*, also give νp and $\bar\nu p$ cross-sections very similar to the model I.

The predictions for $\langle y\rangle_{\bar\nu}$ are shown in figure 5b. The original parametrisation (solid line) shows a marginal increase of $\sim$4% over the 30–200 GeV region, whereas the modified parametrisation (dashed line) gives a practically flat value. Both are compatible with the CIT data or with the CDHS data, taking into account its acceptance error. We have not shown the $\langle y\rangle_\nu$ result, since the data are meagre (in view of the acceptance error on CDHS points being much bigger here).

2.3. *Low Q^2 scale breaking*

The effects of including low Q^2 scale breaking are shown by dotted lines in figures 3–7. Comparing the solid and dotted lines in figures 3 and 4, one sees that this effect reduces the cross-sections appreciably in the low energy end leaving them practically unaltered on the high energy end. The reason simply is that the low Q^2 scale breaking (incorporated in analogy with the *ep* data (Stein *et al* 1975)) truncates the cross-section at $Q^2 \sim 0$. Since a larger part of the cross-sections comes from this region at lower energies, the result follows. Note also that in the $Q^2 \sim 0$ (i.e. $xy \sim 0$) region the σ_ν and $\sigma_{\bar\nu}$ are equal. Thus the low Q^2 scale breaking effect reduces the two cross-sections by the same amount, which can be seen from figures 3 and 4. As a consequence, the ratio R is appreciably reduced in the low energy end, with a much smaller change at the high energy end (figure 2). Thus this effect enhances the rise of R. This is quite appreciable even over the 30–200 GeV range. For instance, it increases the AFT prediction of a 7–8% rise to $\sim$14%, as shown in figure 2a. One also sees from figure 2a (dotted line) that such a faster rise is still compatible with the CDHS data, while it improves the agreement with the BEBC and CIT points. Moreover one sees from figure 4a that the incorporation of the low Q^2 scale breaking brings the AFT prediction on $\sigma_{\bar\nu}/E$ to much closer agreement with the BEBC and CIT data. Corresponding prediction for σ_ν/E becomes flat over the 30–200 GeV (figure 3a), but this is certainly compatible with the BEBC and CIT data. There is only one uncomfortable discrepancy, which is with the low energy Gargamelle points for the individual cross-sections (figures 3a and 4a). The relative position of these Gargamelle points vis-a-vis the rest suffers, however, from the normalisation uncertainties as discussed earlier. Thus, if we ignore the Gargamelle point, the remaining data seem to be fitted better by AFT with the low Q^2 scale breaking included than plain AFT. The effect makes only small difference to $\langle y \rangle$ or $\langle y \rangle_{\bar\nu}$ (figure 5a) whereas its effect on $\sigma_\nu - \sigma_{\bar\nu}$ and P is imperceptible (figures 6, 7). The predictions of the phenomenological scale breaking model with low Q^2 effect are very similar, particularly if one uses the modified parametrisation of (A.21).

2.4. *Longitudinal cross-section*

The effect of a nonzero longitudinal cross-section, incorporated through (A.27) and (A.28), are shown by the dot dashed lines of figures 2–8. It pushes up the magnitude of the quantities $\sigma_{\nu,\bar\nu}/E$ without affecting their energy dependence, as one sees by comparing the dotted and the dot dashed curves on figures 3, 4. The amount added to σ_ν and $\sigma_{\bar\nu}$ (expression A.27) are almost equal as one sees from (A.5). Thus the effect pushes up the ratio R, without again affecting its energy dependence (figure 2). It has only a very small effect on $\langle y \rangle_{\nu,\bar\nu}$ whereas that on the quantities $(\sigma_\nu - \sigma_\nu)$ or P is again imperceptible. Comparison with the data of figures 3 and 4 shows that in spite of the large error bars of the BEBC and the CIT data, they clearly disfavour such a large longitudinal contribution. Note that the longitudinal contribution alone (i.e. without the low Q^2 scale breaking effect), would make the disagreement even worse.

2.5. *SU(3) breaking*

We have studied the effect of SU(3) breaking in the sea along with the low Q^2 scale

breaking. For this we simply suppress the strange quark component in the sea by a factor of 2. The resulting predictions for R and $\sigma_{\nu,\bar{\nu}}/E$ are shown in figures 2a to 4e by long dashes (to be compared with the dotted lines). It reduces $\sigma_{\nu,\bar{\nu}}$ by the same amount, but the effect goes away below the charm threshold due to the Cabibbo suppression. As a result the scale breaking in R is slightly reduced (by $\sim$1%). It has no perceptible effect on the other quantities of interest (see also Fox 1978). Its effect on model II are very similar, and therefore have not been shown separately.

Finally it is interesting to note that the plain AFT prediction for R can be effectively faked by a model with only low Q^2 scale breaking (triangles in figure 2a). Each predicts a 7–8% rise in R over the 30–200 GeV range. But their predictions for σ_ν/E are opposite. Thus the two scale breaking effects add up in R giving a 14% rise for the dotted line in figure 2a and cancel in σ_ν/E giving a flat dotted line in figure 3a. Therefore a precise measurement of these two quantities can help a good deal to disentangle the two scale breaking effects. This is significant in view of the difficulty in binning the neutrino data in Q^2.

3. Conclusion

Let us conclude with a list of lessons learnt from this exercise.

(1) The AFT scale breaking (Buras and Gaemers 1978) (model I) predicts a slow rise for the ratio R of $\sim$7–8% over the 30–200 GeV range. This is insensitive to the scale breaking parameter or the gluon distribution. A rise of $\sim$14% suggested by the BGP approximation (Barnett *et al* 1976) (model IA) has little quantitative significance as the model fails to fit the scale breaking in *ep* data. The phenomenological scale breaking (Perkins *et al* 1977) (model II) gives even a slower rise of $\sim$4–5% for R, which is insensitive to the details of parametrisation. Inclusion of the low Q^2 scale breaking, in analogy with the *ep* data (Stein *et al* 1975) roughly doubles the AFT rise (R rises by $\sim$14%). Inclusion of a longitudinal cross-section, again in analogy with the *ep* data (Barger and Phillips 1978), pushes up the magnitude of R (by $\sim$15%), without affecting the energy dependence. The SU(3) breaking effect reduces the rise—but only marginally.

(2) AFT predicts a σ_ν/E decreasing by $\sim$6% over this region, and a practically flat $\sigma_{\bar{\nu}}/E$, which are again insensitive to the scale breaking parameter or the gluon distribution. The phenomenological model suggests an increase for both σ_ν/E and $\sigma_{\bar{\nu}}/E$, which is sensitive, however, to the details of the parametrisation. With a modified parametrisation, designed to resemble the AFT results for *ep*, the $\sigma_{\nu,\bar{\nu}}$ also turn out to be very similar to those of AFT. The low Q^2 scale breaking gives a rising contribution to σ_ν/E and $\sigma_{\bar{\nu}}/E$, which cancels the AFT decrease in the former and makes the latter rise by $\sim$12%. Inclusion of the longitudinal contribution again pushes up the magnitudes of $\sigma_{\nu,\bar{\nu}}/E$ appreciably without affecting its energy dependence. The SU(3) breaking effect reduces these quantities somewhat, again without affecting the energy dependence, above 40 GeV.

(3) The plain AFT predictions are compatible with the recent neutrino data in the 30–200 GeV region for R and σ_ν, but for $\sigma_{\bar{\nu}}$ there is an uncomfortable discrepancy. Inclusion of low Q^2 scale breaking improves the agreement with these data appreciably particularly for $\sigma_{\bar{\nu}}$. Inclusion of the longitudinal contribution, on the other

hand, goes the wrong way. The data seem to suggest against such a large longitudinal contribution.

(4) Since the AFT and the low Q^2 scale breaking effects are almost equal in R and opposite in σ_ν/E, careful measurements of these two quantities can help to disentangle the two sources of scale breaking.

(5) The AFT and the phenomenological scale breaking models predict $\langle y \rangle_{\nu,\bar{\nu}}$ that are practically flat (to within $\sim$2%) and insensitive to the parameters of the models (again within $\sim$2%). The inclusion of the low Q^2 scale breaking and longitudinal contribution has only a small effect on these predictions. The predictions agree with the limited data available on these quantities*.

Acknowledgements

We gratefully acknowledge computational help from Mr Ashok Raina and discussions with Drs Probir Roy and K V L Sarma.

Appendix

(a) Formalism

Following the current practice, we study scale breaking within the framework of a quark parton model. We shall only be concerned with isoscalar target and with charged current cross-sections. For this case, we have, in the convention of Barger and Phillips (1974)

$$\frac{d^2\sigma_{\nu,\bar{\nu}}}{dQ^2 d\nu} = \frac{d^2\sigma_{\nu,\bar{\nu}}}{dxdy}/(2MyE^2) = \frac{G^2ME}{\pi}\left[F_2^{\nu,\bar{\nu}}\left(1-y-\frac{Mxy}{2E}+\frac{y^2}{2}\right)\right.$$

$$\left.\mp xF_3^{\nu,\bar{\nu}}\left(y-\frac{y^2}{2}\right)\right]/(2MyE^2), \tag{A.1}$$

where $G^2M/\pi = 1{\cdot}53 \times 10^{-38}$ cm^2/GeV. (A.2)

Here M is the target nucleon mass, E is the incident neutrino energy, and ν and Q^2 are the energy and four momentum square transferred between the two. In terms of these

$$x = \frac{Q^2}{2M\nu},\quad y = \frac{\nu}{E} \text{ and } W^2 = M^2 + 2MEy(1-x), \tag{A.3}$$

where W is the invariant mass of the final state hadron. The eq. (A.1) above assumes, of course, the Callan-Gross relation

$$xF_1 = F_2, \tag{A.4}$$

*On completion of this work we got a preprint from Buras and Gaemers (Buras and Gaemers 1977) who have considered the plain AFT (model I) predictions for neutrino scattering. The other aspects of our analysis are not covered, however.

i.e. a zero longitudinal to transverse cross-section ratio. This follows in a quark parton model or in an AFT (to leading order), and has been assumed in all the models considered here. Therefore, we shall start with this assumption. However the effect of a finite longitudinal to transverse cross-section ratio will be considered below.

The above structure functions are related to the quark distributions, via

$$F_2^p = x[2v(\cos^2\theta_C+\sin^2\theta_C\cdot\theta(W-W_C))+4\xi+(2\xi+2\xi_C)\,\theta(W-W_C)];$$

$$xF_3^p = -x[2v(\cos^2\theta_C+\sin^2\theta_C\cdot\theta(W-W_C)+(2\xi-2\xi_C)\,\theta(W-W_C)];$$

$$F_2^{\bar\nu} = x[2v+4\xi+(2\xi+2\xi_C)\cdot\theta(W-W_C)];$$

$$xF_3^{\bar\nu} = -x[2v-(2\xi-2\xi_C)\cdot\theta(W-W_C); \tag{A.5}$$

where $\sin^2\theta_C=0{\cdot}05$ is the Cabibbo angle and charm excitation has been incorporated through a fast rescaling theta function (Barger 1975) with a threshold $W_C=4$ GeV. Here $v=(v_u+v_d)/2$ and denotes the charge averaged valence contribution and ξ denotes the SU(3) symmetric sea, and ξ_C the charm $(C\bar C)$ component in the sea. In a scaling model these quantities are functions of x only. These have been parametrised by Barger and Phillips (1974) as

$$v_u = 0{\cdot}594\,x^{-1/2}(1-x^2)^3+0{\cdot}461\,x^{-1/2}(1-x^2)^5+0{\cdot}621\,x^{-1/2}(1-x^2)^7;$$

$$v_d = 0{\cdot}072\,x^{-1/2}(1-x^2)^3+0{\cdot}206\,x^{-1/2}(1-x^2)^5+0{\cdot}621\,x^{-1/2}(1-x^2)^7;$$

$$\xi = 0{\cdot}145\,x^{-1}(1-x)^9; \tag{A.6}$$

using the SLAC data (Bodek *et al* 1973) on $\nu W_2^{ep,n}$ $(=F_2^{ep,n})$. This will be taken as the low Q^2 input in the phenomenological scale breaking models below. By all evidence, the charm component ξ_C is strongly suppressed (Sivers 1976) at low Q^2. It is, indeed, common practice to start with a zero value (Altarelli 1976; Barnett *et al* 1976; Buras and Gaemers 1978). For consistency with charm photoproduction (Roy 1977) we shall take

$$\xi_C = 0{\cdot}014\,\xi = 0{\cdot}002\,x^{-1}(1-x)^9, \tag{A.7}$$

instead of zero, in the range $Q^2\sim$1–2 GeV^2. Of course, this makes little difference to the output.

One should note that the above parametrisation (A.6) is a fit to the data over different ranges of Q^2 at different x, as suggested by (A.3). It corresponds to a

$$Q^2 \sim 15x. \tag{A.8}$$

The variation of average Q^2 with x is significant, in view of the scale breaking observed in the SLAC range itself (Riordon *et al* 1975). Using

$$\nu W_2^{ep} = x\left[\frac{4}{9}v_u+\frac{1}{9}v_d+\frac{4}{3}\xi+\frac{8}{9}\xi_C\right], \tag{A.9}$$

one can, in fact, check that the parametrisation (A.6) reproduces the SLAC structure function (Riordon *et al* 1975) for a given x (figure 1) over only a limited Q^2 range around the corresponding $\langle Q^2 \rangle$.

(*b*) *AFT scale breaking* (*model I*)

The AFT, to leading order, prescribes the following Q^2 dependence for the moments of the distribution functions $v^l = \int_0^1 v x^l dx$, etc. For the first moments (Altarelli 1976; Barnett *et al* 1976; Hinchliffe and Llewellyn Smith 1977; Gluck and Reya 1976; Buras and Gaemers 1978).

$$v^1(Q^2) = v^1(L)^{-32/75};$$

$$\xi^1(Q^2) = \frac{1}{4}\left[\frac{3}{14} + \left(3\xi^1 + v^1 + \xi^1{}_C - \frac{3}{14}\right) L^{-56/75} + (\xi^1 - \xi^1{}_C - v^1)\, L^{-32/75}\right];$$

$$\xi^1{}_C(Q^2) = \frac{1}{4}\left[\frac{3}{14} + \left(3\xi^1 + v^1 + \xi^1{}_C - \frac{3}{14}\right) L^{-56/75} - (3\xi^1 - 3\xi^1{}_C + v^1)\, L^{-32/75}\right] \tag{A.10}$$

where the moments on the right hand side are evaluated at a moderately low $Q^2 = Q_0^2$, and

$$L = \ln (Q^2/\Lambda^2)/\ln (Q_0^2/\Lambda^2), \tag{A.11}$$

being the scale breaking parameter. For the 2nd moments

$$v^2(Q^2) = v^2\, L^{-2/3};$$

$$\xi^2(Q^2) = \frac{1}{4}[0_1{}^2(Q^2) + (\xi^2 - \xi^2{}_C - v^2)\, L^{-2/3}];$$

$$\xi^2{}_C(Q^2) = \frac{1}{4}[0_1{}^2(Q^2) - (3\xi^2 - 3\xi^2{}_C + v^2)\, L^{-2/3}]; \tag{A.12}$$

where the singlet operator

$$0_1{}^2(Q^2) = [0{\cdot}925(3\xi^2 + \xi^2{}_C + v^2) + 0{\cdot}144\, G^2]\, L^{-0{\cdot}609} + [0{\cdot}075\,(3\xi^2 + \xi^2{}_C + v^2) - 0{\cdot}144\, G^2]\, L^{-1{\cdot}386}, \tag{A.13}$$

G^2 being the 2nd gluon moment. The corresponding singlet operator for the 1st moment was much simpler due to the fact that the 1st gluon moment is simply related to the 1st quark moments by momentum conservation.

The above relations, of course, do not still give the Q^2 dependence of the distribution function, we shall, however, use the approximation of Buras and Gaemers

(1978), who have shown that the sea contributions, being restricted to the very low x region; can be approximated in terms of the first two moments. That is

$$x\xi(x, Q^2) = \xi^1(Q^2)\left[\frac{\xi^1(Q^2)}{\xi^2(Q^2)} - 1\right]\cdot(1-x)^{\left[\frac{\xi^1(Q^2)}{\xi^2(Q^2)}-2\right]} \tag{A.14}$$

and identically for ξ_C. For the valence part, of course, one has to consider more moments. They are able to reproduce the Q^2 dependence of the first 12 moments with the empirical formula

$$xv(x, Q^2) = \frac{1{\cdot}5x^{(0{\cdot}7-0{\cdot}176\ln L)}(1-x)^{2{\cdot}6+0{\cdot}8\ln L}}{B(0{\cdot}7-0{\cdot}176\ln L,\ 3{\cdot}6+0{\cdot}8\ln L)} \tag{A.15}$$

where the beta function downstairs is to ensure the zeroeth moment sum rule. We shall use their $\Lambda=0.3$ and $Q_0^2=1.8$ and their input moments [all fitted to the electron and muon structure functions (Riordon *et al* 1975; Anderson *et al* 1976, 1977)]

$$\xi^1 = 0{\cdot}018,\quad \xi^2 = 0{\cdot}1528\times10^{-2},\quad G^2 = 0{\cdot}0335;$$

$$v^1 = 0{\cdot}244,\quad v^2 = 0{\cdot}0785. \tag{A.16}$$

These differ slightly from the moments of parametrisation[16] (A.6) above. Instead of their precisely zero input for $\xi_C{}^{1,2}$ we shall use the values of (A.7), which of course make negligible difference to the output.

Evidently, the only parameters, which are not determined by the low $Q^2(\sim Q_0^2)$ data are the scale breaking parameter and the gluon moment G^2. These are determined by the observed scale breaking in the electron and muon data (Riordon *et al* 1975; Anderson *et al* 1976, 1977). To check the sensitivity of the neutrino scattering results on these parameters we shall repeat the calculations with $G^2 = 0{\cdot}057$ [corresponding to a gluon distribution $\sim(1-x)^5$ instead of $(1-x)^{10}$] and also with a $\Lambda=0{\cdot}5$. The latter represents the maximal value of the scale breaking parameter allowed by the electron and muon data.*

(*c*) *Phenomenological scale breaking (model II)*

Perkins *et al* (1977) have shown that the scale breaking in electron (muon) scattering on both proton and isoscalar target can be described in terms of a simple form factor

$$F_2(Q^2, x) = F_2(Q_0^2, x)\cdot(Q^2/Q_0^2)^{0{\cdot}25-x}. \tag{A.17}$$

With the same form factor they were also able to describe the earlier vp and vN data. Since these four processes correspond to different combinations of the valence and the sea quark distributions, the model amounts to assuming the same form factor for all the distributions functions, i.e.

$$v_{u,d}(x, Q^2) = v_{u,d}(x, Q_0^2)\cdot(Q^2/Q_0^2)^{0{\cdot}25-x} \tag{A.18}$$

*Some fits to the electron and muon data, which use the scaling variable ξ instead of x, give $\Lambda = 0{\cdot}5$ as the best value (De Rujula *et al* 1977; Fox 1977).

and identically for the ξ and ξ_C. We shall use the parametrisation of (A.6) and (A.7) for the low Q^2 input on the right hand side. The variation of the effective Q^2 with x in this parametrisation will be taken care of by reexpressing the above equations as

$$v_{u,d}(x, Q^2) = v_{u,d}[x, Q_1^2(x)] \cdot [Q^2/Q_1^2(x)]^{0.25-x}, \text{ etc.} \tag{A.19}$$

where $Q_1^2(x)$ is the average Q^2 for this parametrisation for a given x (eq. (A.8)). We take

$$Q_1^2(x) = 4(x/0.3) = 13.3x \tag{A.20}$$

subject to a minimum 1·8 GeV²—the minimum Q^2 value used in this fit.

To check the sensitivity of the neutrino scattering predictions on the lattitude allowed by the *ep* data, we shall also show these predictions, for an alternative parametrisation

$$v_{u,d}(x, Q^2) = v_{u,d}[x, Q_1^3(x)] \cdot [Q^2/Q_1^2(x)]^{0.075-0.5x}, \text{ etc.} \tag{A.21}$$

in place of (A. 19). This modification is designed to mimic the model I result for the *ep* structure function. Thus, one can see the difference between the two model predictions for neutrino scattering, starting with the same *ep* input. The main difference, we feel, is that the two models distribute the scale breaking in the *ep* structure function, differently amongst the quark functions. In particular the sea term is expected to grow less rapidly here than in model I since the growth of the low x structure function is shared between the sea and valence contributions. The other difference—a logarithmic versus a power Q^2 dependence of models I and II—should not affect the neutrino predictions, as the range of Q^2 involved, is not very much larger than in the electron and muon data, to which they have been fitted. In fact, there is a phenomenological model (Karliner and Sullivan 1977), identical to model II but with a logarithmic form factor. Its predictions are very close to those of model II.

(*b*) *Low Q^2 scale breaking*

The prescriptions given above for both types of model, are used to calculate the quark functions down to a $Q^2_{\min}=1.8$ GeV²—the lowest Q^2 value of the SLAC *ep* data (Riordon *et al* 1975), to which they are fitted. Below this the AFT model is not expected to hold. In any case a straight extrapolation of these formulae down to $Q^2=0$, evidently runs into divergence difficulties. Therefore, the Q^2 integrated neutrino cross-sections would be estimated assuming the quark funtions to be Q^2 independent over the region 0 to 1·8, following the standard practice in the literature (Barnett *et al* 1976; Buras and Gaemers 1978).

There is, of course, no justification for this scaling hypothesis in the very low Q^2 region. The structure functions $F_2^{ep,n}$ measured in the $Q^2=0.1$ to 1.8 GeV² range show a rapid drop below 1 GeV².* This has been parametrised in the form (Stein *et al* 1975).

$$F_2^{ep}(x', Q^2) = F_2^{ep}(x') f(Q^2) \tag{A.22}$$

*It must, of course, vanish at $Q^2 = 0$.

using the Bloom-Gilman (Bloom and Gilman 1970) variable

$$\frac{1}{x'} = \frac{1}{x} + \frac{M^2}{Q^2}. \tag{A.23}$$

That is the low Q^2 scale breaking can be factored out as a common form factor $f(Q^2)$ at all x'. Moreover the same form factor can approximately describe the scale breaking in F_2^{en} as well (Stein *et al* 1975). Since the *ep* and *en* stucture functions correspond to different cc mbinations of the valence and sea contributions it implies that either the two contributions have very similar Q^2 dependence or the sea term dominates over this region. In either case the neutrino structure functions should have the same Q^2 dependence, provided, of course, that the quark parton framework makes any sense at such low Q^2 values.* This would be true, for instance, in models which describe the low Q^2 scale breaking in terms of new scaling variables involving the target and the quark masses (De Rujula *et al* 1977; Fox 1977; Choudhury 1976). More significantly such a form factor seems to be suggested by the consistency requirement between the Gargamelle neutrino and the SLAC electron structure functions (Perkins 1975). In any case, we think, in the absence of any other guidance it is useful to assume a similar Q^2 dependence for the neutrino structure function as that observed for *ep*, *n* and try to estimate the magnitude of scale breaking involved. We shall therefore use the above form factor $f(Q^2)$ to describe the neutrino structure function in the $Q^2 < 1{\cdot}8$ GeV^2 region. The $f(Q^2)$ has been given (Stein *et al* 1975) in terms of the elastic *ep* form factor, and can be written out using the dipole approximately as

$$f(Q^2) = 1 - \left(\frac{1+7{\cdot}8\, Q^2/4M^2}{1+Q^2/4M^2}\right) \cdot (1+Q^2/0{\cdot}71)^{-4} \tag{A.24}$$

which is $\simeq 1$ for $Q^2 \geqslant 1{\cdot}8$. The scaling factor $F_{2,3}(x')$ corresponding to the structure functions at $Q^2 \geqslant 1{\cdot}8$, can be obtained from the quark distributions in x', also given in Barger and Phillips (1974). These are (compare (A.6)).

$$xv = 0{\cdot}225x'^{1/2}(1-x'^2)^3 + 0{\cdot}063x'^{1/2}(1-x'^2)^5 + 1{\cdot}035x'^{1/2}(1-x'^2)^7;$$

$$x\xi = 0{\cdot}132\,(1-x')^9. \tag{A.25}$$

(e) *Longitudinal cross-section*

We shall now consider the effect of a nonzero longitudinal to transverse cross-section ratio

$$R = \frac{F_2}{xF_1} - 1. \tag{A.26}$$

*The F_2 structure function in neutrino scattering is expected to be similar to the F_2^{ep} on more general grounds like CVC, chiral symmetry and isovector dominance of photon. Although chiral symmetry would breakdown for $Q^2 \lesssim m_\pi^2$, it should be a reasonable approximation in the bulk of the $Q^2 \lesssim 1{\cdot}8$ GeV^2 region.

This is incorporated simply by adding a term

$$\left(\frac{G^2ME}{\pi}\right)\cdot[RxF_1^{\nu,\bar{\nu}}\cdot(1-y)]/(2MyE^2), \tag{A.27}$$

to the right hand side of eq. (A.1). A recent measurement from SLAC (1977) gives a value $R=0{\cdot}35\pm0{\cdot}16$ over a wide range of x and Q^2, whereas an earlier measurement (Riordon *et al* 1975) gave $R\sim0{\cdot}15$ over a similar range with equally large error bars. Using an average of the two values and the constraint that R must vanish at $Q^2=0$, it has been parametrised by Barger and Phillips (1978) as

$$R = 0{\cdot}25\ Q^2/(Q^2+m^2). \tag{A.28}$$

We shall use this parametrisation and assume the same R for the neutrino case. Again the $Q^2\to0$ limit of the neutrino R is very different from the electron case, as one can see from PCAC. We shall ignore, however, this low Q^2 correction to R since R is itself a correction term. We should only mention that this amounts, if at all, to an underestimation of the longitudinal contribution.

References

Altarelli G 1976 *Proceedings of the XI Recontre de Moriond* ed Tran Van Tham (Orsay: CNRS
Anderson H *et al* 1976 *Phys. Rev. Lett.* **37** 4
Anderson H *et al* 1977 *Phys. Rev. Lett.* **38** 1450
Barger V and Phillips R J N 1974 *Nucl. Phys.* **B73** 269
Barger V 1975 Lectures given at McGill International Summer School, Wisconsin Preprint
Barger V and Phillips R J N 1978 *Nucl. Phys.* **B132** 531
Barish B C *et al* 1977 *Phys. Rev. Lett.* **20** 1313
Barnett R M, Georgi H and Politzer H D 1976 *Phys. Rev. Lett.* **20** 1313
Benevenuti A *et al* 1976 *Phys. Rev. Lett.* **37** 189
Bloom E D and Gilman F J 1970 *Phys. Rev. Lett.* **25** 1140
Bodek A *et al* 1973 *Phys. Rev. Lett.* **30** 1087
Bosetti P C *et al* 1977 *Phys. Lett.* **70B** 273
Buras A J and Gaemars K J F 1977 *Phys. Lett.* **B71** 106
Buras A J and Gaemers K J F 1978 *Nucl. Phys.* **B132** 249
Choudhury D K 1976 TIFR Preprint (to appear in *Phys. Rev.*)
De Rujula A, Georgi H and Politzer H D 1977 *Ann. Phys.* **103** 315
Fox G C 1977 *Nucl. Phys.* **B131** 107
Fox G C 1978 *Nucl. Phys.* **B134** 269
Gluck M and Reya E 1976 *Phys. Lett.* **B64** 169
Hinchliffe I and Llewellyn Smith C H 1977 *Phys. Lett.* **B66** 281
Holder H *et al* 1977 *Phys. Rev. Lett.* **39** 433
Karliner I and Sullivan J D 1977 University of Illinois, Urbana Preprint (unpublished).
Lederman L *et al* 1977 *Phys. Rev. Lett.* **39** 252
Perkins D H 1975 *Proceedings of SLAC Lepton Photon Conference*
Perkins D H *et al* 1977 *Phys. Lett.* **B67** 347
Riordon E M *et al* 1975 SLAC-PUB-1634
Roy D P 1977 *Phys. Lett.* **B68** 76 and TIFR Preprint
Sivers D 1976 *Nucl. Phys.* **B106** 95
Stein S *et al* 1975 *Phys. Rev.* **D12** 1884
SLAC Results 1977 Presented at Hamburg International Conference